

RESEARCH

Open Access



The injury effect of osteopontin in sepsis-associated lung injury

Qian Wang^{1,2,3,4}, Zhicai Yu^{5,6}, Zhixin Song^{2,3,4,7}, Xue Lu^{1,2,3,4}, Zhu Li^{2,3,4,8}, Dandan Pi^{1,2,3,4}, Jing Li^{1,2,3,4,9*} and Feng Xu^{1,2,3,4,9*}

Abstract

Background Sepsis is a severe condition causing organ failure due to an abnormal immune reaction to infection, characterized by ongoing excessive inflammation and immune system issues. Osteopontin (OPN) is secreted by various cells and plays a crucial role in inflammatory responses and immune regulation. Nonetheless, the precise function of OPN in sepsis remains to be elucidated.

Methods In the present study, we evaluated the levels of OPN in paediatric patients with sepsis and healthy individuals. We examined the impact of OPN on survival rates, systemic inflammation, and lung injury within an experimental sepsis model using cecal ligation and puncture (CLP). Furthermore, the pro-inflammatory effects and potential mechanisms of OPN in sepsis were investigated through Mouse Hemophagocytic Synuclein (MH-S) cells.

Results The OPN level was found to be elevated in patients with sepsis (368.5 ± 249.4 ng/ml) compared to children with infections (73.78 ± 40.46 ng/ml) ($p < 0.0001$) and healthy individuals (44.03 ± 20.76 ng/ml) ($p < 0.0001$). The serum concentration of OPN was elevated in pediatric patients with septic shock compared to those with sepsis (504 ± 266.3 ng/ml vs. 238.6 ± 143.8 ng/ml, $p < 0.001$). Intravenous administration of OPN inhibitor into the tail vein decreased the mortality rate (HR = 0.2695, $p = 0.0015$), suppressed systemic inflammatory responses and mitigated lung tissue damage. The concentration of tumour necrosis factor (TNF)- α , IL-6 and IL-1 β in serum of CLP mice treated with OPN inhibitor decreased compared with CLP mice. Within the sepsis mouse model, there was a marked increase in OPN expression in the lung's tissues compared to the sham group mice. This surge was accompanied by a significant accumulation of alveolar macrophages and an upregulation of inflammasome expression. Mechanistic investigations in MH-s cells revealed that OPN-siRNA suppressed the LPS-induced macrophage inflammatory response by inhibiting caspase-1-dependent classical pyroptosis signaling pathway. However, recombinant OPN was supplemented after OPN silencing, the protective effects in MH-s cells treated with LPS were reversed.

Conclusion This study reveals that OPN has an adverse impact on the host's immune response to sepsis. Suppressing OPN expression holds potential therapeutic value for the treatment of sepsis.

Trial registration Study on the diagnostic value of osteopontin in children with sepsis. MR5024001771. Registered 22 January 2024. <https://www.medicalresearch.org.cn>.

*Correspondence:

Jing Li
lijingwangyi@126.com
Feng Xu
xufeng9899@163.com

Full list of author information is available at the end of the article



© The Author(s) 2025. **Open Access** This article is licensed under a Creative Commons Attribution-NonCommercial-NoDerivatives 4.0 International License, which permits any non-commercial use, sharing, distribution and reproduction in any medium or format, as long as you give appropriate credit to the original author(s) and the source, provide a link to the Creative Commons licence, and indicate if you modified the licensed material. You do not have permission under this licence to share adapted material derived from this article or parts of it. The images or other third party material in this article are included in the article's Creative Commons licence, unless indicated otherwise in a credit line to the material. If material is not included in the article's Creative Commons licence and your intended use is not permitted by statutory regulation or exceeds the permitted use, you will need to obtain permission directly from the copyright holder. To view a copy of this licence, visit <http://creativecommons.org/licenses/by-nc-nd/4.0/>.

Keywords Sepsis, Lung injury, Osteopontin, Macrophage pyroptosis

Introduction

Sepsis is defined as life-threatening organ dysfunction caused by a dysregulated host response to infection [1]. Sepsis-associated lung injury is the most common severe organ dysfunction in children with sepsis, significantly contributing to elevated morbidity and mortality rates [2, 3]. The latest diagnostic criteria for sepsis in children emphasize the high incidence and importance of respiratory dysfunction, especially as a secondary organ dysfunction [4]. Research has revealed that 25 million cases of sepsis in children were reported in 2017, which resulted in over 3 million deaths [5]. Despite numerous clinical investigations into sepsis and lung injury, identifying effective therapeutic drugs remains a formidable challenge.

Osteopontin (OPN), also known as early T lymphocyte activation 1 protein, and secreted phosphorylated protein 1 (SPP1), is a member of the family of small integrin-binding ligand N-linked glycoproteins. It exists in various forms and fragments, with a molecular weight ranging from 41 to 74 kilodaltons (kDa) [6, 7]. OPN is secreted by a wide range of tissue cells throughout the body and plays a crucial role in inflammatory response and immune regulation [8–11]. Previous studies have found that OPN concentrations are significantly elevated in the serum of patients with sepsis [12]. Currently, the precise role and mechanism of OPN in sepsis remain to be clarified.

To explore the potential role of OPN in sepsis, we first assessed serum OPN levels in pediatric patients diagnosed with the condition. Subsequently, we established a mouse model of sepsis through cecal ligation and puncture (CLP), and a cellular model of sepsis by co-culturing lipopolysaccharide (LPS) with mouse hemophagocytic synuclein (MH-S) cells, to examine the function and potential molecular mechanisms of OPN in the context of sepsis.

Materials and methods

Study population

Serum samples were obtained from children fulfilling the inclusion criteria and hospitalized at the Children's Hospital of Chongqing Medical University from January 2024 through December 2024. A total of 43 cases of sepsis were included, with the following criteria: a. Consistency with the 2024 International Consensus on Sepsis in Children [4]. During the same period, 28 cases of infected children were identified among children exhibiting signs of infection, yet these cases did not meet the diagnostic criteria for sepsis within the same age group at the same hospital. For the control group, consisting of 38 healthy children, the subjects were of the same age and

were examined at the same hospital's health examination center during a physical examination.

This study protocol has received approval from the Institutional Review Board of Children's Hospital of Chongqing Medical University (File No: (2021) Ethical Review Research No. 325-1). Informed consent has been obtained from all participants in accordance with the principles outlined in the Declaration of Helsinki.

Experimental animals

Male wild-type (WT) C57BL/6J mice, aged between 6 and 8 weeks, were procured from Chongqing Medical University. These mice were bred in a controlled environment characterized by a temperature range of 20–24 °C and a 12-hour light/dark cycle. They were provided with unrestricted access to standard food and water. All animal experiments were conducted in compliance with the regulations approved by the Chongqing Experimental Animal Center and the Animal Committee of Children's Hospital (Approval No.: CHCMU-IACUC20231208004).

To create a model of polymicrobial sepsis, the CLP procedure was performed [13]. Mice were anesthetized using pentobarbital sodium at a dosage of 50 mg/kg. After sterilization, a 1-cm midline laparotomy was performed on the abdomen, the cecum was then ligated at 20% of its length and punctured with an 18-gauge needle, resulting in a slight extrusion of cecal contents. Subsequently, the cecum was repositioned into the abdominal cavity, and the incisions were sutured. Sham-operated animals underwent identical surgical procedures, except for the ligation and puncture of the cecum. After CLP surgery, the animals were resuscitated with an intraperitoneal injection of normal saline at a ratio of 1 ml per 20 g of body weight. Twenty-four hours post-surgery, the animals were humanely euthanized, after which serum and lung tissue samples were collected.

Cells experiments

MH-s cells (Procell, Wuhan, China) were cultured in RPMI1640 medium supplemented with 10% fetal bovine serum (FBS) and 1% penicillin-streptomycin, within a 37 °C, 5% CO₂ incubator, and subcultured at intervals of 1 to 2 days. The cells were allocated into three distinct groups: negative control (NC) group, NC+LPS group, and OPN-siRNA + LPS (SiRNA + LPS) group. A concentration of 100nM of either NC or OPN-siRNA was complexed with an equal volume of transfection reagent for 10–15 min. Subsequently, these complexes were added to MH-s cells in RPMI1640 medium supplemented with 10% FBS and incubated for a period ranging from 24 to 72 h. Then, the medium was refreshed, and 100 ng/mL

LPS was introduced to continue the culture for an additional 6 h. Ultimately, RNA or protein was extracted from the cells.

Inhibitor-mediated blockade of OPN

To counteract the activity of OPN in CLP, mice in the CLP + OPN inhibitor (OI) group were administered 50 μ g of an OPN inhibitor (MCE, OPN expression inhibitor 1, HY-146064, USA), which was dissolved in 100 μ l of phosphate buffered saline (PBS). In contrast, a control group of mice received an equivalent volume of sterile PBS as a vehicle control.

In vitro administration of recombinant OPN

Prior to treatment, MH-s cells were subjected to OPN knockdown via OPN-siRNA transfection. The cells were then divided into two groups: the experimental group, which was treated with 200 ng/mL of recombinant mouse OPN (rmOPN) protein (MCE, Osteopontin, HY-P78358, USA) for 30 min, and the control group, which received no such treatment. Both groups were subsequently co-cultured with 100 ng/mL of LPS for 6 h. Ultimately, cell supernatant, RNA and protein were extracted from the cells.

Enzyme-linked immunosorbent assay (ELISA)

The concentrations of OPN in human samples were quantified by using commercial ELISA kits provided by FineTest (EH0248, China), and serum inflammatory factor IL-6 was quantified using Human IL-6 ELISA kit (Neobioscience, EHC007, China). Likewise, the levels of OPN (Jonin, JL10068, China) and various inflammatory cytokines in mice (with $n=5-8$ per group) were evaluated. These cytokines encompassed tumor necrosis factor- α (TNF- α) (Neobioscience, EMC102a.96, China), interleukin (IL)-1 β (Neobioscience, EMC001b.96, China), and IL-6 (Neobioscience, EMC004.96, China). Both serum and cell supernatant samples were analyzed with commercially available ELISA kits.

The dry-to-wet (D/W) ratio of lung tissue

The upper lobe of the right lung from the mice was excised. The blood on its surface was carefully absorbed using filter paper and then it was weighed. This weight was recorded as the wet weight (W). Subsequently, the tissue was placed in an oven set at 60 $^{\circ}$ C for a duration of 48 h. After that, it was weighed again, and the result was noted as the dry weight (D). Consequently, the dry-to-wet ratio of the lung tissue was calculated using the formula D/W.

Immunofluorescence detection

The paraffin sections of lung tissue were heated at 60 $^{\circ}$ C in an oven for 1 h. Subsequently, dewaxing and sodium

citrate antigen retrieval were performed. Then, the sections were cooled and rinsed three times with 1 \times phosphate-buffered saline with tween-20 (PBST) for 5 min each. Incubation with goat serum was performed at room temperature for 30 min. After drying the slides, they were placed in a humid chamber with the primary antibody and incubated overnight at 4 $^{\circ}$ C. The primary antibodies employed were as follows: anti-Osteopontin (Abcam, ab283656, USA), NLRP3 Monoclonal antibody (Proteintech, 68102-1-Ig, China) and F4/80 Rat mAb (zenbio, 263101, China). On the next day, the slides were washed again with 1 \times PBST three times for 5 min each. Then, the secondary antibodies such as CoraLite 488-conjugated Goat Anti-Rabbit IgG (H+L), Fluorescein (FITC)-conjugated Goat Anti-Mouse IgG (H+L) (Proteintech, SA00003-1, China) and Rabbit anti-Rat IgG H&L (FITC) (zenbio, 550066, China) were then added and incubated at room temperature in the dark for 1 h. After washing three times with 1 \times PBST as before, a drop of 4',6-diamidino-2-phenylindole(DAPI)-containing anti-fluorescence quenching mounting medium was applied to seal the slides, and images were captured using a fluorescence microscope.

Histopathology

Lung tissue was harvested, and hematoxylin and eosin (H&E) staining was utilized to evaluate pathological changes ($n=5$). Fresh samples were rinsed with cold PBS and then fixed in 4% paraformaldehyde. Subsequently, the tissues were dehydrated, embedded in paraffin, sliced into 4 μ m sections, and stained routinely. The pathology scores for the lung were determined based on the following aspects: alterations in lung histology, such as edema, congestion, interstitial inflammation, and inflammatory cell infiltration.

RNA extraction and quantitative real-time PCR

Total RNA was extracted from cells by employing the RNA Isolation Kit (Beyotime, R0027, China). Subsequently, 1 μ g of RNA was reverse transcribed into cDNA using the ABScript III RT Master Mix for qPCR, which includes a gDNA remover kit (ABclonal, RK20429, China). Gene expression was analyzed through real-time quantitative PCR (qPCR) on a Bio-Rad CFX ConnectTM Real-Time System (Bio-Rad, USA), utilizing SYBR Green (ABclonal, Rk21203, China). The primer sequences are detailed in Table 1. The expression levels were quantified using the 2 $^{-\Delta\Delta Cq}$ method, with glyceraldehyde-3-phosphate dehydrogenase (GAPDH) serving as the internal control.

Western blotting analysis

Proteins were extracted from cells by using a radio-immunoprecipitation assay (RIPA) lysis buffer (MCE,

Table 1 q-PCR primer sequences. OPN osteopontin, TNF tumour necrosis factor, IL interleukin, NLRP3 NOD-, LRR- and pyrin domain-containing 3, GSDMD Gasdermin D, ASC apoptosis-associated speck-like protein containing a CARD, GAPDH glyceraldehyde-3-phosphate dehydrogenase, siRNA small interfering RNA, qPCR quantitative real-time reverse transcriptase-polymerase chain reaction, siRNA small interfering RNA

Primer	Sequence
OPN	F-5'-TGACGATGATGATGACGATGGAGAC-3' R-5'-TGTAGGGACGATTGGAGTGAAAGTG-3'
TNF- α	F-5'-CACGCTCTTCTGCTACTGAACTTC-3' R-5'-CTTGGTGGTTTGTGAGTGTGAGG-3'
IL-6	F-5'-TTCTTGGGACTGATGCTGGTGAC-3' R-5'-GTGGTATCCTCTGTGAAGTCTCCTC-3'
IL-1 β	F-5'-CTCGCAGCAGCACATCAACAAG-3' R-5'-CCACGGGAAAGACACAGGTAGC-3'
NLRP3	F-5'-AGGAGGAAGAAGAAGAGAGGAGAGG-3' R-5'-TTGAGAAGAGACCACGGCAGAAG-3'
GSDMD	F-5'-GTGGACAGCTGCGGAATC-3' R-5'-GGTCTGGTTCTGGAGCACTGG-3'
caspase1	F-5'-CCTGGTCTTGACTTGGAGGAC-3' R-5'-ATCAGCAGTGGGCATCTGTAGC-3'
ASC	F-5'-GAAGTGGACGGAGTCTGGATG-3' R-5'-ATCTTGCTTGGCTGGTGTCTC-3'
IL-18	F-5'-AAAGTGCCAGTGAACCCAGAC-3' R-5'-AGAGAGGGTACAGCCAGTCC-3'
GAPDH	F-5'-GCAAATCAACGGCACAGTCAAG-3' R-5'-TCGCTCCTGGAAGATGGTGATG-3'
OPN-siRNA	F-5'-GGAUGUGAUCGAUAGUCAATT-3' R-5'-UUGACUAUCGAUCAUCCTT-3'

HY-K1001, USA) supplemented with 1% phenylmethanesulfonyl fluoride (PMSF) (MCE, HY-B0496, USA), 1% protease inhibitor (MCE, HY-K0010, USA), and 1% phosphatase inhibitors (MCE, HY-K0021, USA). The protein concentration was quantified using a NanoDrop spectrophotometer (Thermo Fisher). Subsequently, the proteins were separated by sodium dodecyl sulfate-polyacrylamide (SDS-PAGE) gel (EpiZyme Biotechnology, PG112, China) electrophoresis and then transferred onto a polyvinylidene fluoride (PVDF) membrane (Millipore, IPVH00010, USA). The membranes were blocked with NcmBlot blocking buffer (New Cell & Molecular Biotech, P30500, China) for 20 min and incubated with the appropriate primary antibodies overnight at 4 °C. The primary antibodies employed were as follows: anti-Osteopontin (Abcam, ab283656, USA), anti-IL-1 β (Proteintech, 16806-1-AP, China), anti-IL-18 (Proteintech, 10663-1-AP, China), NLRP3 Rabbit mAb (Abclonal, A24294, China), GSDMD Polyclonal antibody (Proteintech, 20770-1-AP, China), CASP1 Rabbit pAb (Abclonal, A20470, China), ASC Rabbit mAb (Abclonal, A22046, China), anti-IL-6 (MCE, HY-P80723, USA), anti-TNF- α (Proteintech, 17590-1-AP, China) and beta Actin Rabbit mAb (zenbio,

R23613, China). Thereafter, the membranes were incubated with goat anti-rabbit IgG, HRP-conjugated polyclonal antibody (CoWin Bio, CW0103S, China) and goat anti-mouse HRP-conjugated polyclonal antibody (Proteintech, 66009-1-Ig, China) as secondary antibodies at room temperature for 1 h, and the results were visualized using a Bio-Rad ChemiDoc™ Touch Imaging System (Bio-Rad, California, USA).

Statistical analysis

Statistical analyses were performed using GraphPad Prism 9 software. All data are presented as the mean \pm standard deviation (SD) from at least three independent experiments. Group differences were evaluated by either a t-test (Mann-Whitney U test) or a one-way analysis of variance (Tukey's multiple comparison test). A P value less than 0.05 was considered statistically significant, where "n" values indicate the number of cultures, tissue samples, or animals examined within each group.

Results

The concentration of OPN is significantly elevated in pediatric patients with sepsis

In the present study, ELISAs were employed to confirm the expression of OPN. The detailed characteristics of patients diagnosed with sepsis, infection, and healthy controls are outlined in Table 2. The serum concentration of OPN was observed to be increased in pediatric patients with sepsis (368.5 ± 249.4 ng/ml) compared to both healthy individuals (44.03 ± 20.76 ng/ml) ($p < 0.0001$) and those with infections (73.78 ± 40.46 ng/ml) ($p < 0.0001$) (Fig. 1A). Furthermore, the serum concentration of OPN was elevated in pediatric patients with septic shock compared to those with sepsis (504 ± 266.3 ng/ml vs. 238.6 ± 143.8 ng/ml, $p < 0.001$) (Fig. 1B). In addition, we found that the serum OPN level on the first day (243.5 ± 204.3 ng/ml) was significantly higher than that on the second day (69.58 ± 58.70 ng/ml) ($p < 0.005$) and the third day (60.42 ± 55.15 ng/ml) ($p < 0.005$) in pediatric patient with sepsis admission to PICU (Fig. 1C). It is noteworthy that this trend exhibited a positive correlation with the concentration of the serum inflammatory cytokine IL-6 in patients concurrently (Fig. 1D).

The OPN expression is elevated in the plasma and lungs following septic mice

To analyze variations in OPN levels at the 24-hour mark after CLP, serum and lung tissues from both Sham and CLP mice were analyzed using ELISA and immunofluorescence techniques. The ELISA results indicated a significant elevation of OPN in the serum of CLP mice compared with the Sham group (0.7312 ± 0.2263 vs. 0.3765 ± 0.08419 ng/ml, $p = 0.0001$) (Fig. 2A), mirroring observations in septic patients. Correspondingly,

Table 2 Characteristics of paediatric patients with sepsis, infections and healthy controls

Characteristics	Sepsis patients (n = 43)	Infection patients (n = 28)	healthy controls (n = 38)
Sex (male/female)	23/20	14/14	22/16
Age (years)	4.81(1.00-6.25)	4.44(1.35-7.25)	7.09(5.00-9.44)
CRP (mg/L)	78.60(18.88-127.8)	12.34(3.615-19.35)	NA
PCT (ng/ml)	32.92(1.29-68.12)	0.28(0.075-0.27)	NA
IL-6(pg/ml)	2656(51.94-3009)	NA	NA
IL-10(pg/ml)	287.9(44.24-461.1)	NA	NA
TNF- α (pg/ml)	1.528(0.575-2.145)	NA	NA
IL-1 β (pg/ml)	22.67(1.365-2.45)	NA	NA
Organs dysfunction(n, %)			
Respiratory	29	NA	NA
Circulatory	16	NA	NA
Nervous	12	NA	NA
Blood	18	NA	NA
Gastrointestinal	12	NA	NA
Urinary	5	NA	NA
Infection site (Number of patients)			
Respiratory	26	22	NA
Gastrointestinal	5	3	NA
Nervous	4	0	NA
Vascular	3	2	NA
Urinary	1	0	NA
Skin	1	1	NA
Bacteraemia Isolates (Number of patients)			
Gram positive	10	NA	NA
Gram negative	12	NA	NA
Mycoplasma pneumonia	7	NA	NA
Fungus	2	NA	NA
Virus	16	NA	NA
Miscellaneous	5	NA	NA
Other	/	NA	NA
Phoenix Sepsis Score	3.4(2-4)	NA	NA
PICU stay(days)	11.74(6-16)	NA	NA
Ventilation	31	NA	NA
Died/survived	4/39	NA	NA

The data are expressed as the median (interquartile range) unless otherwise indicated. CRP C-reactive protein, PCT procalcitonin, IL interleukin, TNF tumour necrosis factor, PICU paediatric intensive care unit, NA not applicable

immunofluorescence analysis showed that, compared with the Sham group, the expression of OPN in the lung tissue of the CLP group increased by 34.8%, $p = 0.0039$ (Fig. 2BC).

Administration of OPN inhibitor protects septic mice

To elucidate the function of OPN in the development of sepsis, mice subjected to CLP were administered an OPN expression inhibitor 1. Notably, the survival rate of these CLP mice was increased (HR = 0.2695, $p = 0.0015$) (Fig. 3A). This protective outcome might be ascribed to a diminished systemic inflammatory response following the onset of sepsis. We observed that compared with the Sham group, the levels of serum inflammatory factors in CLP mice were significantly increased, and the OPN

expression inhibitor 1 significantly reversed this change, such as IL-6 (17.17 ± 9.543 pg/ml vs. 661.5 ± 513.3 pg/ml vs. 125.1 ± 160.5 pg/ml), TNF- α (9.486 ± 10.21 pg/ml vs. 158.2 ± 86.98 pg/ml vs. 25.52 ± 9.279 pg/ml), and IL-1 β (16.62 ± 7.695 pg/ml vs. 33.41 ± 3.282 pg/ml vs. 25.25 ± 1.541 pg/ml) (Fig. 3B).

Administration of OPN inhibitor protects against sepsis-associated lung injury in mice

To elucidate the impact of the OPN expression inhibitor 1 on CLP-associated lung injury, we initially conducted a histological examination of lung tissue and evaluated the extent of injury using a standardized scoring system, as detailed in the Materials and Methods section. Representative histological images of lung tissue

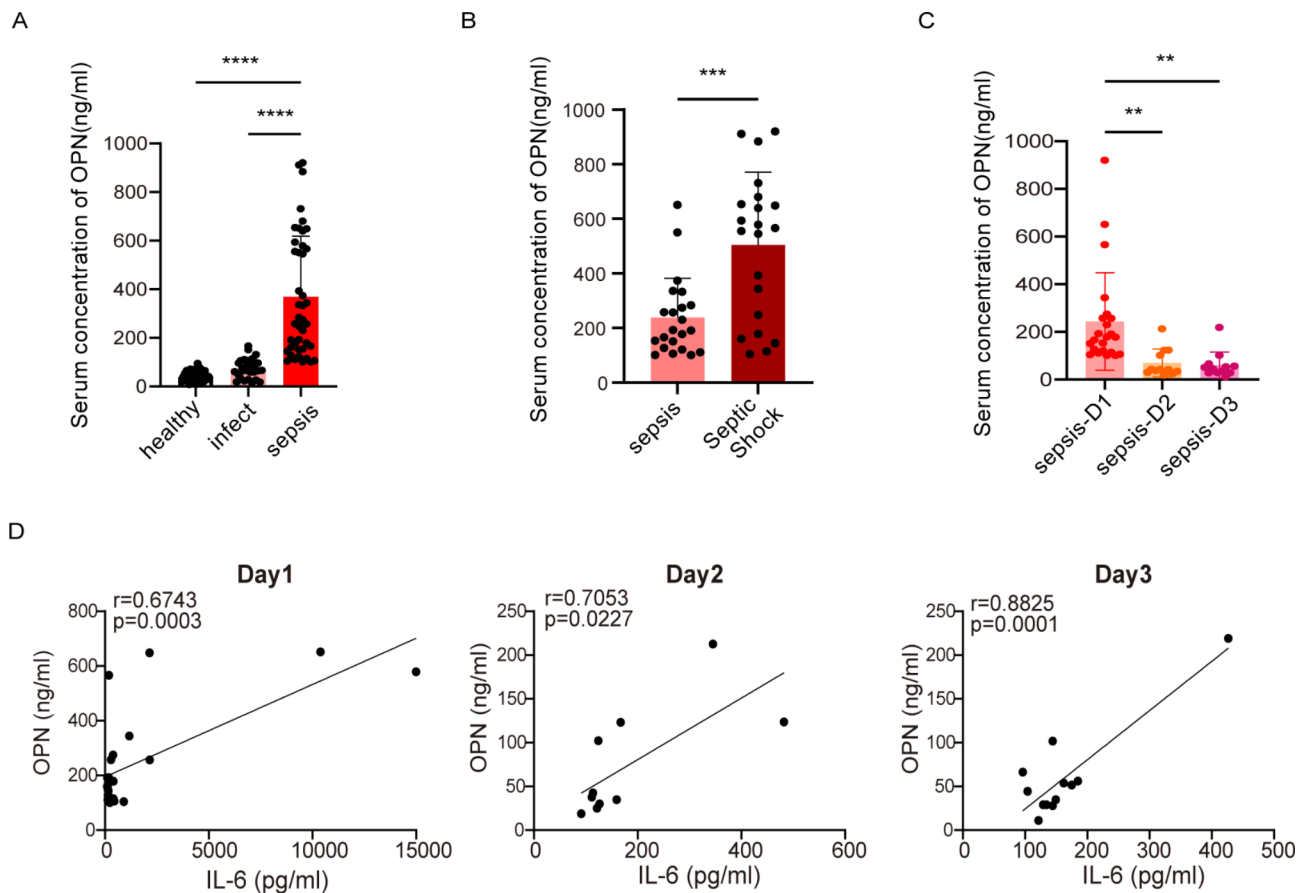


Fig. 1 OPN levels are significantly elevated in pediatric patients with sepsis. **(A)** ELISAs were used to confirm the expression of OPN in 43 paediatric patients with sepsis, 38 healthy controls, and 28 common infections in clinical studies. **(B)** Serum levels of OPN in 43 paediatric patients with sepsis ($n=22$) and septic shock ($n=21$). **(C)** ELISAs was employed to identify the level of OPN in the serum of paediatric patients with sepsis at 1st ($n=23$), 2nd ($n=12$), 3rd ($n=12$) day after staying in PICU. **(D)** The correlation between OPN and IL-6 concentration in the serum of paediatric patients with sepsis at 1st ($n=23$), 2nd ($n=10$), 3rd ($n=12$) day after staying in PICU. The data are presented as the means \pm standard deviations (S.D.). “*” indicates a difference between groups. * $p < 0.05$, ** $p < 0.01$, *** $p < 0.001$, **** $p < 0.0001$. Osteopontin, OPN; interleukin, IL; The first day of pediatric patient with sepsis admission to PICU, sepsis-D1; The second day of pediatric patient with sepsis admission to PICU, sepsis-D2; The third day of pediatric patient with sepsis admission to PICU, sepsis-D3; enzyme-linked immunosorbent assay, ELISA

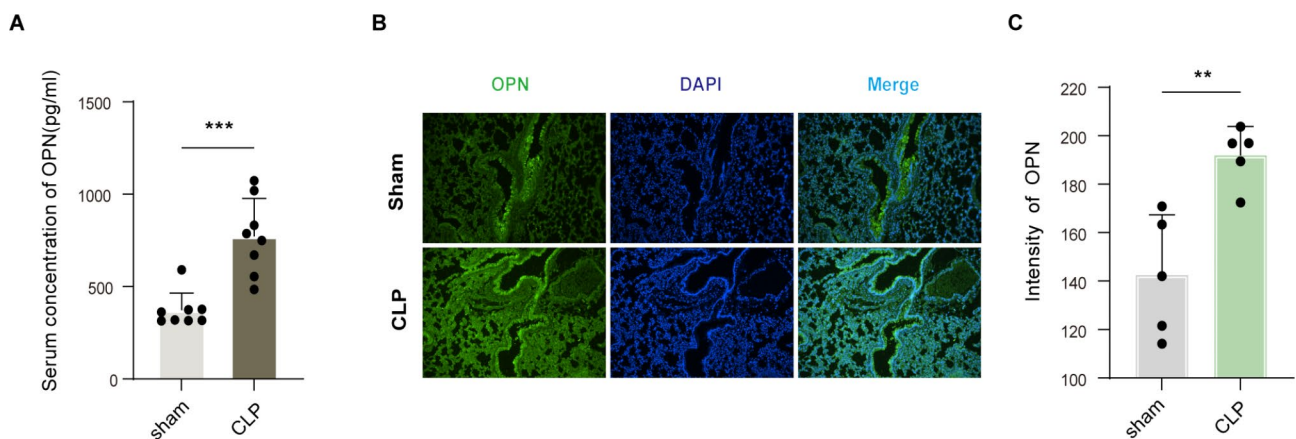


Fig. 2 The expressions of OPN are improved obviously in mice with CLP. **(A)** Serum levels of OPN in sham mice and mice with CLP ($n=8$). **(B)** Immunofluorescence was employed to detect the expression of OPN in lung tissue ($n=5$). **(C)** Relative fluorescence intensity of OPN in the lung tissue of Sham and CLP mice. The data are presented as the means \pm standard deviations (S.D.). “*” indicates a difference between groups. * $p < 0.05$, ** $p < 0.01$, *** $p < 0.001$, **** $p < 0.0001$. Osteopontin, OPN; caecal ligation and puncture, CLP; 4',6-diamidino-2-phenylindole, DAPI

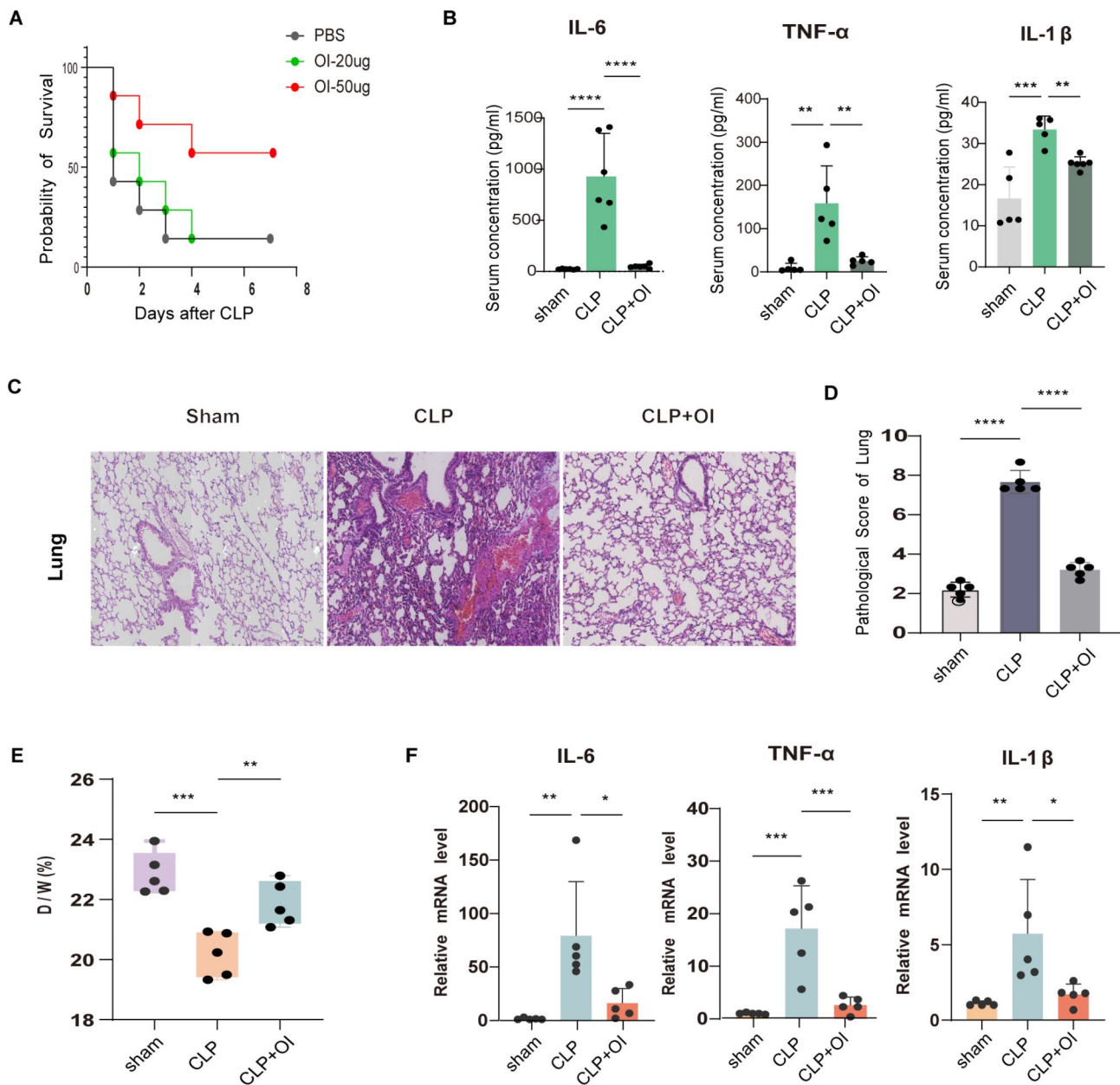


Fig. 3 Administration of OPN inhibitor protects septic mice. **(A)** Survival of mice with CLP after treatment with OPN inhibitor ($n=12$). **(B)** Serum cytokine levels in the Sham, CLP and CLP+OPN inhibitor groups at 24 h post-operative ($n=5-6$). **(C)** Lung tissues were stained with H&E in the Sham, CLP and CLP+OPN inhibitor groups ($n=5$). **(D)** Semiquantitative scores of lung tissues were calculated in the Sham, CLP and CLP+OPN inhibitor groups ($n=5$). **(E)** The D/W ratio of lung tissue in the Sham, CLP and CLP+OPN inhibitor groups ($n=5$). **(F)** The mRNA expression levels of IL-6, TNF- α and IL-1 β in lung tissues were determined by qPCR ($n=5$). The data are presented as the means \pm standard deviations (S.D.). *** indicates a difference between groups. * $p < 0.05$, ** $p < 0.01$, *** $p < 0.001$, **** $p < 0.0001$. Osteopontin, OPN; OPN inhibitor, OI; caecal ligation and puncture, CLP; phosphate buffered saline, PBS; interleukin, IL; tumour necrosis factor, TNF; haematoxylin-eosin staining, HE; dry-to-wet, D/W; Quantitative Real-time reverse transcriptase-polymerase chain reaction, qPCR

from mice treated with sham surgery, vehicle, and OPN inhibitor are depicted in Fig. 3C. Compared with the sham group, the lung tissue from the CLP group exhibited pronounced morphological alterations, including edema, hemorrhage, alveolar collapse, and infiltration of inflammatory cells. Conversely, treatment with OPN inhibitors markedly attenuated these microscopic signs

of deterioration when compared to the CLP group. As illustrated in Fig. 3D, the histological injury score of lung tissue was significantly higher in the CLP group than the sham group (7.667 ± 0.5774 vs. 2.200 ± 0.3801 , $p < 0.0001$), whereas the OPN inhibitor-treated group exhibited a significant improvement in the histological injury score compared to the vehicle group (3.200 ± 0.3801 vs.

7.667 ± 0.5774 , $p < 0.0001$). Subsequently, we assessed the D/W ratio of lung tissue in mice. Our findings indicated that the D/W ratio in the CLP group was markedly lower than that of the sham-operated group ($20.18\% \pm 0.7485\%$ vs. $22.85\% \pm 0.7066\%$, $p = 0.0002$); however, the administration of the OPN expression inhibitor 1 effectively reversed this trend ($21.85\% \pm 0.7329\%$ vs. $20.18\% \pm 0.7485\%$, $p = 0.0065$) (Fig. 3E). Beyond blood analysis, we also evaluated the expression of cytokines in lung tissue at the mRNA level. The levels of IL-6, TNF- α , and IL-1 β in lung tissue were considerably elevated in the vehicle group compared to the sham group. Nevertheless, treatment with an OPN inhibitor resulted in a significant reduction of these mRNA levels by 80%, 87.5%, and 70%, respectively, compared to the vehicle mice (Fig. 3F). The pathological sections of mouse lung tissue in this study revealed a substantial infiltration of inflammatory cells following CLP, with OPN inhibitors markedly decreasing their count. However, macrophages constitute the primary immune cells within the lungs. Certain studies suggest that OPN facilitates the migration of macrophages to areas of disease, although there remains a divergence of views on whether OPN exerts pro-inflammatory or anti-inflammatory effects. So, we first examined changes in the number of macrophage infiltrates by F4/80 staining. Immunofluorescence staining showed greater infiltration of F4/80-positive macrophages into lung tissue in the CLP group than in the sham group, and OPN inhibitors significantly reduced the number of F4/80-positive macrophages. Interestingly, we observed the same trend of NOD-, LRR- and pyrin domain-containing 3 (NLRP3) inflammasome in lung tissue (Fig. 4ABC). This may elucidate the precise mechanism through which OPN mediates its deleterious effects on the lungs.

OPN aggravates macrophage inflammatory response in vitro

To elucidate the role of OPN in sepsis-associated lung injury in mice, we investigated the impact of OPN-siRNA on LPS-treated MH-s cells in vitro. Initially, we identified the presence of OPN in the supernatant of LPS-stimulated MH-s cells and the mRNA expression of OPN in the control group. Our findings indicated that both the mRNA (6.761 ± 1.241 vs. 1.211 ± 0.1833 , $p = 0.0016$) (Fig. 5A) and protein (2139 ± 1186 pg/ml vs. 349.8 ± 60.05 pg/ml, $p = 0.0236$) (Fig. 5B) levels of OPN were markedly elevated following LPS stimulation compared to the control group. Then, we successfully employed OPN-siRNA to suppress the expression of OPN at both the mRNA and intracellular and extracellular protein levels in MH-s cells (Fig. 5CDE). Subsequently, we found that both the mRNA and protein levels of IL-6, TNF- α and IL-1 β in MH-s cells were increased during LPS exposure, while silencing OPN could significantly reduce their levels

(Fig. 6AB). This outcome further substantiates the pro-inflammatory and tissue-damaging role of OPN within the context of a sepsis model at the cellular level.

OPN promotes pyroptosis in macrophages treated with LPS

Pyroptosis, as a form of programmed cell death, plays a crucial role in initiating and advancing the inflammatory response through an amplification loop of inflammation and necrosis [14]. In vivo experiments, we observed that OPN inhibitor can significantly reduce the expression of NLRP3 in the lungs of CLP mice, we hypothesize that there is a correlation between OPN and pyroptosis. We silenced the expression of OPN in MH-s cells, and then detected the expression of NLRP3, Gasdermin D (GSDMD), caspase1, apoptosis-related spot-like protein (ASC), IL-1 β and IL-18. The results showed that silencing OPN expression significantly reduced both the mRNA and protein levels of NLRP3, GSDMD, caspase1, ASC, IL-1 β and IL-18 in the LPS-induced pyroptosis pathway (Fig. 7AB).

Administration of rmOPN after OPN silencing, the protective effects in MH-s cells treated with LPS were reversed.

To further elucidate the role of OPN in the inflammatory response, MH-s cells were subjected to OPN knockdown via OPN-siRNA transfection prior to experimentation. Then, rmOPN was added and co-cultured with LPS. after OPN silencing, the supplementation of rmOPN reversed the protective effects. We first detected the concentrations of IL-6 and TNF- α in the cell supernatant. The results showed that the supplement of rmOPN could significantly increase the expression levels of IL-6 and TNF- α in LPS-induced MHs cells following OPN knockdown (Fig. 8A). Subsequently, we detected the mRNA and protein levels of pyroptosis pathway proteins. The results showed that both mRNA and protein levels of NLRP3, GSDMD, caspase1, ASC, IL-1 β and IL-18 were significantly increased in LPS-induced MHs cells after OPN silencing (Fig. 8BC). Overall, these results indicate that the OPN-mediated inflammatory response in MH-S cells is facilitated by the induction of caspase1-dependent classical pyroptosis.

Discussion

The findings revealed that circulating levels of OPN were significantly elevated in children with sepsis compared to healthy group and infections group, and there is a certain correlation with the severity of sepsis. Additionally, the administration of OPN inhibitors in septic mice demonstrated that survival rates were increased by suppressing the expression of inflammatory mediators (TNF- α , IL-1 β , IL-6) and mitigating tissue damage, at least in the lung tissue. Moreover, vitro

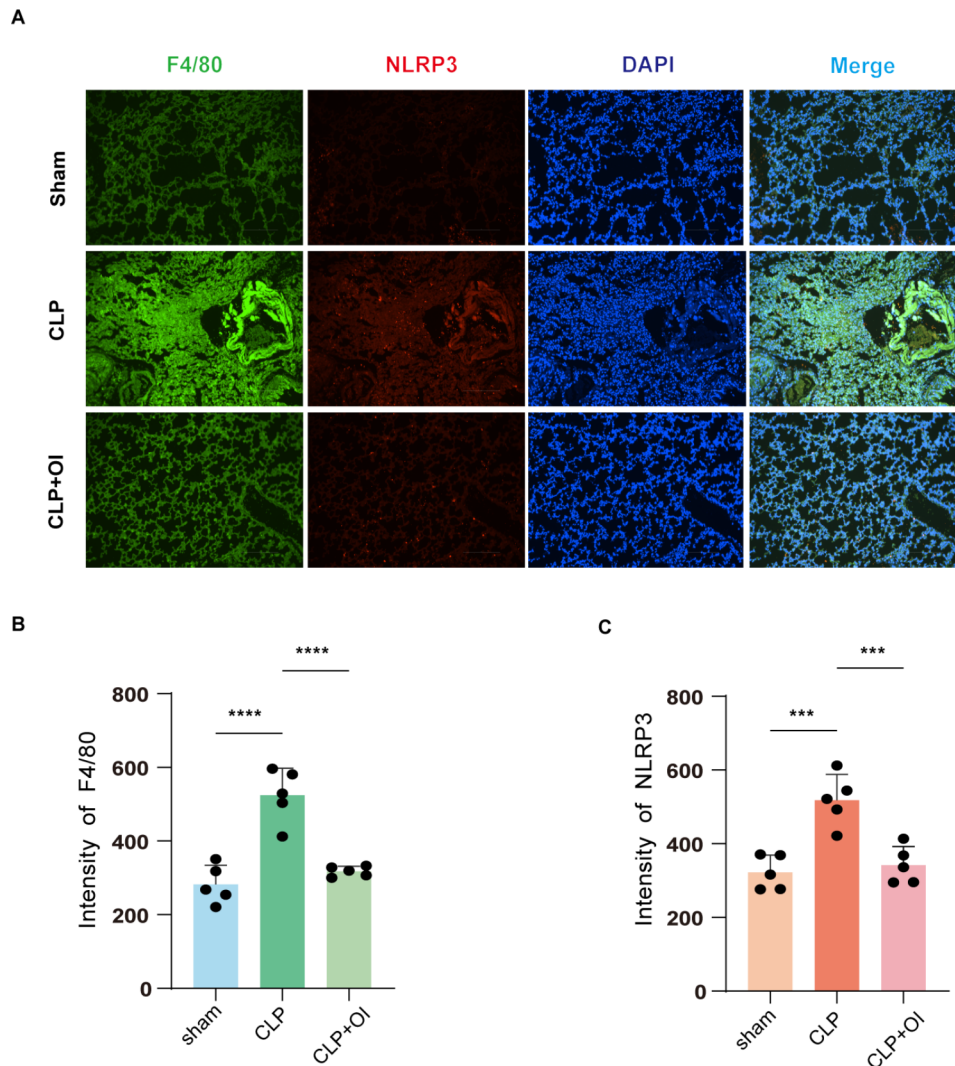


Fig. 4 Administration of OPN inhibitor reduced macrophage infiltration and inflammasome expression in lung tissue. **(A)** Immunofluorescence was employed to detect the expression of F4/80 and NLRP3 in lung tissue ($n=5$). **(B)** Relative fluorescence intensity of F4/80 in the lung tissue of Sham, CLP and CLP + OPN inhibitor groups. **(C)** Relative fluorescence intensity of NLRP3 in the lung tissue of Sham, CLP and CLP + OPN inhibitor groups. The data are presented as the means \pm standard deviations (S.D.). **** indicates a difference between groups. * $p < 0.05$, ** $p < 0.01$, *** $p < 0.001$, **** $p < 0.0001$. Osteopontin, OPN; OPN inhibitor, OI; NOD-, LRR- and pyrin domain-containing 3, NLRP3; 4',6-diamidino-2-phenylindole, DAPI; caecal ligation and puncture, CLP

experiments indicated that the silencing of OPN expression curtailed the inflammatory response by inhibiting the pyroptosis signaling pathway in LPS-stimulated MH-s cells, and administration of rmOPN after OPN silencing, the protective effects in MH-s cells treated with LPS were reversed.

Federico Carbone and colleagues discovered that elevated early OPN levels can forecast mortality in patients suffering from septic shock, and the OPN levels on the first day are associated with multiple organ dysfunction, prolonged hospital stays, extended durations for resolving infections, and various pro-inflammatory responses mediated by macrophages [15]. Additionally, research has indicated that plasma OPN detection could diagnose sepsis in patients [16]. However, these investigations have

primarily concentrated on adult subjects, with limited data available on pediatric septic patients. In our study, we observed that the serum OPN levels in children with sepsis were significantly higher than those in patients with infections and healthy controls, and the serum concentration of OPN was elevated in pediatric patients with septic shock compared to those with sepsis. We also observed that the serum OPN levels on the first day were notably elevated compared to the second day and the third day among survivors of sepsis in the PICU. Furthermore, this trend exhibited a positive correlation with the concentration of the serum inflammatory cytokine IL-6 in patients concurrently. The concentration of OPN seems to decrease with the improvement of inflammatory response in children with sepsis.

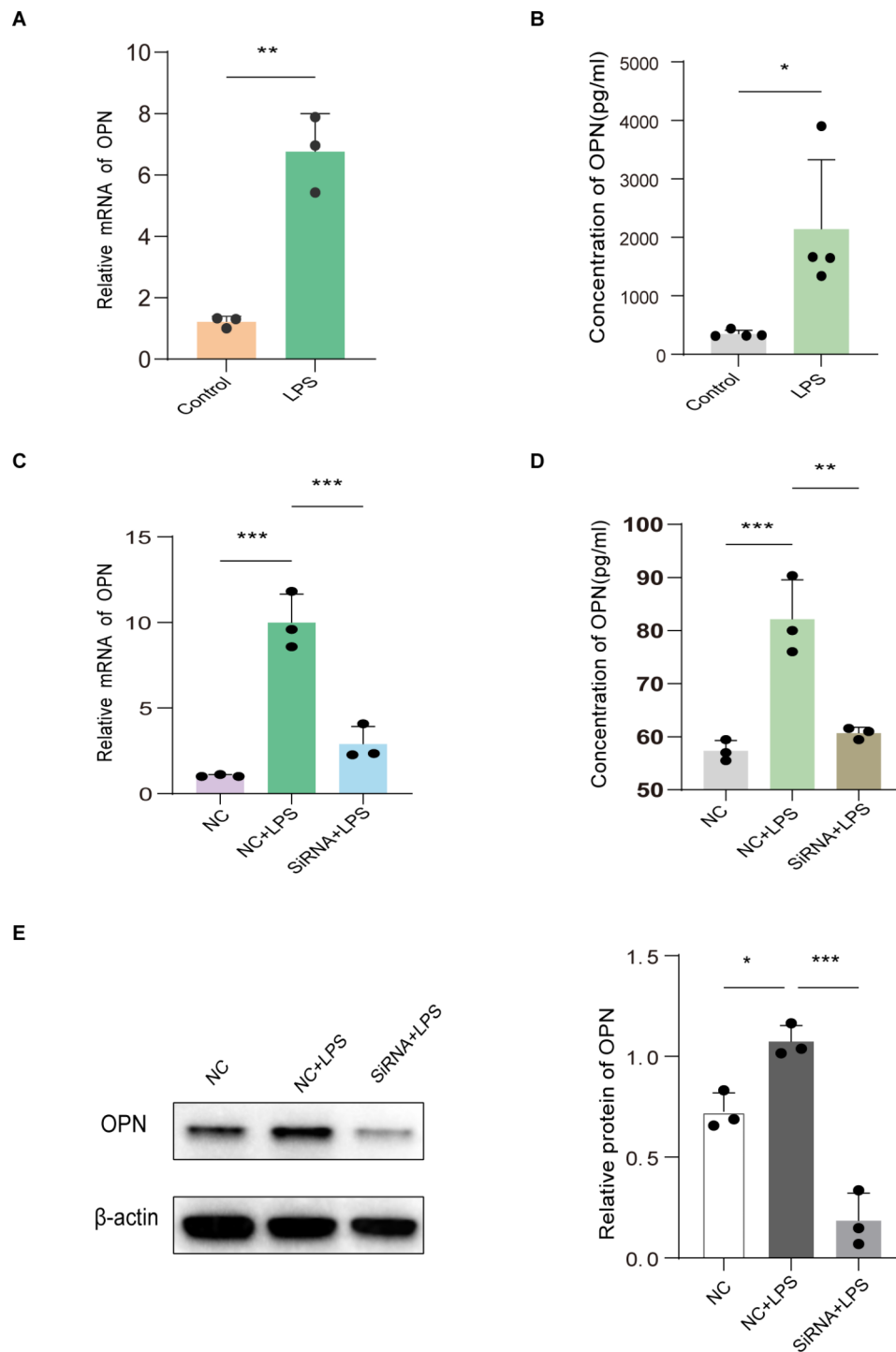


Fig. 5 OPN was increased in LPS-treated MH-s cells, and OPN-siRNA could silence the expression of OPN. **(A)** The mRNA expression levels of OPN in MH-s cells were determined by qPCR. **(B)** ELISAs were used to detect the concentration of OPN in cell supernatant of MH-s cells. **(C)** The mRNA expression levels of OPN in MH-s cells were determined by qPCR. **(D)** ELISAs were used to detect the concentration of OPN in cell supernatant of MH-s cells. **(E)** Western blot analysis of the relative expression levels of OPN in MH-s cells. The data are presented as the means \pm standard deviations (S.D.). “***” indicates a difference between groups. * $p < 0.05$, ** $p < 0.01$, *** $p < 0.001$, **** $p < 0.0001$. Osteopontin, OPN; negative control, NC; Small interfering RNA, SiRNA; lipopolysaccharide, LPS; Mouse alveolar macrophage cells, MH-s; Quantitative Real-time reverse transcriptase-polymerase chain reaction, qPCR; enzyme-linked immunosorbent assay, ELISA

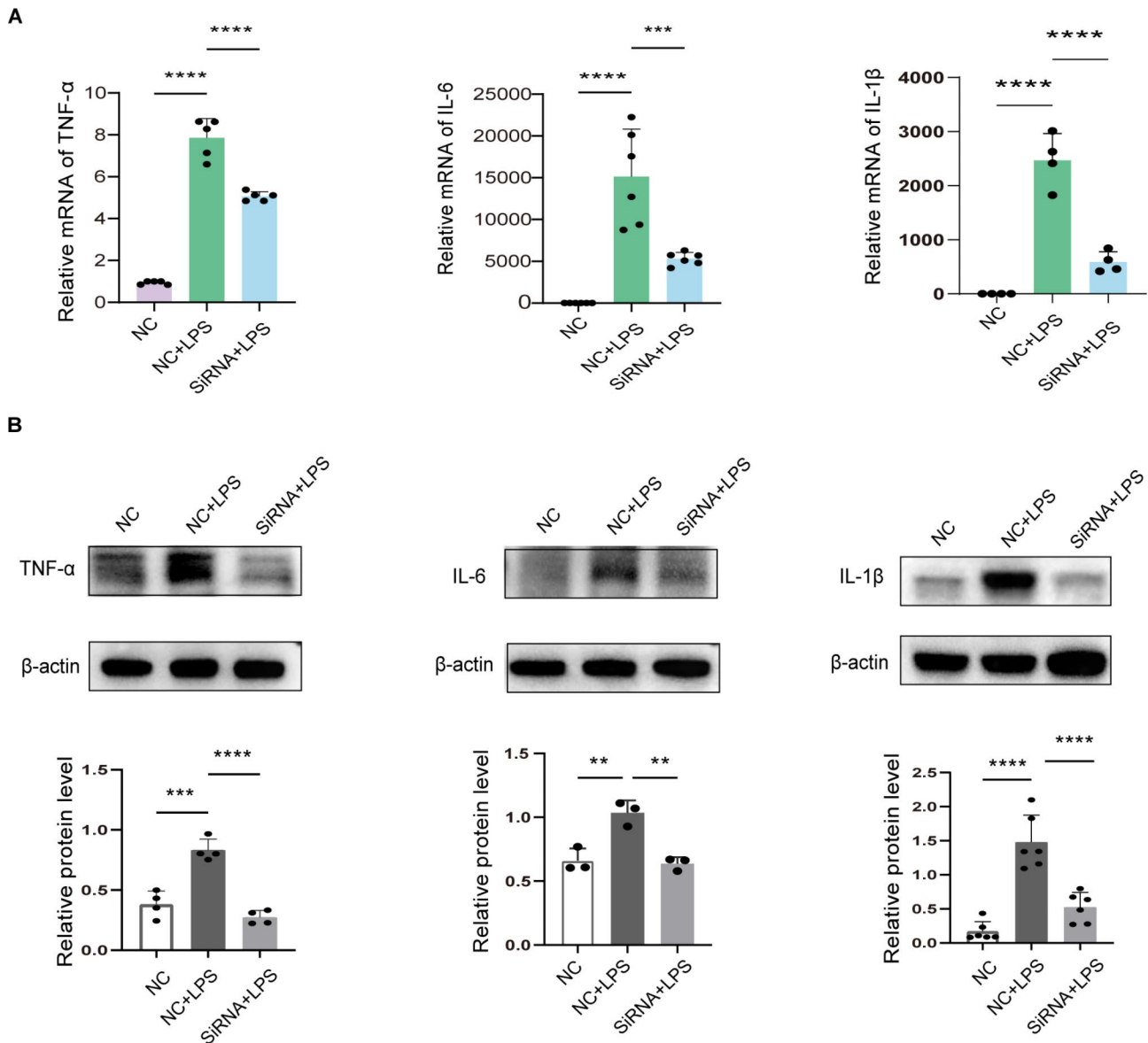


Fig. 6 OPN-siRNA decreases inflammatory cytokine responses in LPS-treated MH-s cells. **(A)** The mRNA expression levels of TNF- α , IL-6 and IL-1 β in MH-s cells were determined by qPCR. **(B)** Western blot analysis of the relative expression levels of TNF- α , IL-6 and IL-1 β in MH-s cells. The data are presented as the means \pm standard deviations (S.D.). *** indicates a difference between groups. * p < 0.05, ** p < 0.01, *** p < 0.001, **** p < 0.0001. Osteopontin, OPN; interleukin, IL; tumour necrosis factor, TNF; negative control, NC; Small interfering RNA, SiRNA; lipopolysaccharide, LPS; Mouse alveolar macrophage cells, MH-s; Quantitative Real-time reverse transcriptase-polymerase chain reaction, qPCR

In vivo experiments, we revealed that mortality, systemic inflammatory response and organ damage were aggravated in CLP, which may be related to the increase in OPN concentration. When treated with an OPN inhibitor, we found that all of those were improved. It is reasonable to infer that the overall improvement in sepsis outcomes through the inhibition of OPN may be attributed to the suppression of systemic inflammation and the amelioration of lung organ damage. Vitro experiments showed a positive correlation between OPN levels and the expression of cytokines TNF- α , IL-6 and IL-1 β in the LPS-induced inflammatory response model of MH-s

cells. The inhibition of OPN expression by using OPN-siRNA was found to counteract the elevation of TNF- α , IL-6 and IL-1 β . These findings support the anti-inflammatory properties of OPN-siRNA.

Bruemmer et al. have demonstrated that acute macrophage infiltration is significantly diminished in OPN^{-/-} mice compared to WT counterparts in a dextran sodium sulfate (DSS)-induced colitis [17]. Then, Yohei et al. discovered that OPN significantly enhanced neutrophil migration to inflammatory lung lesions by upregulating the mitogen-activated protein (MAP) kinase signaling pathway molecules p38 and extracellular signal-regulated

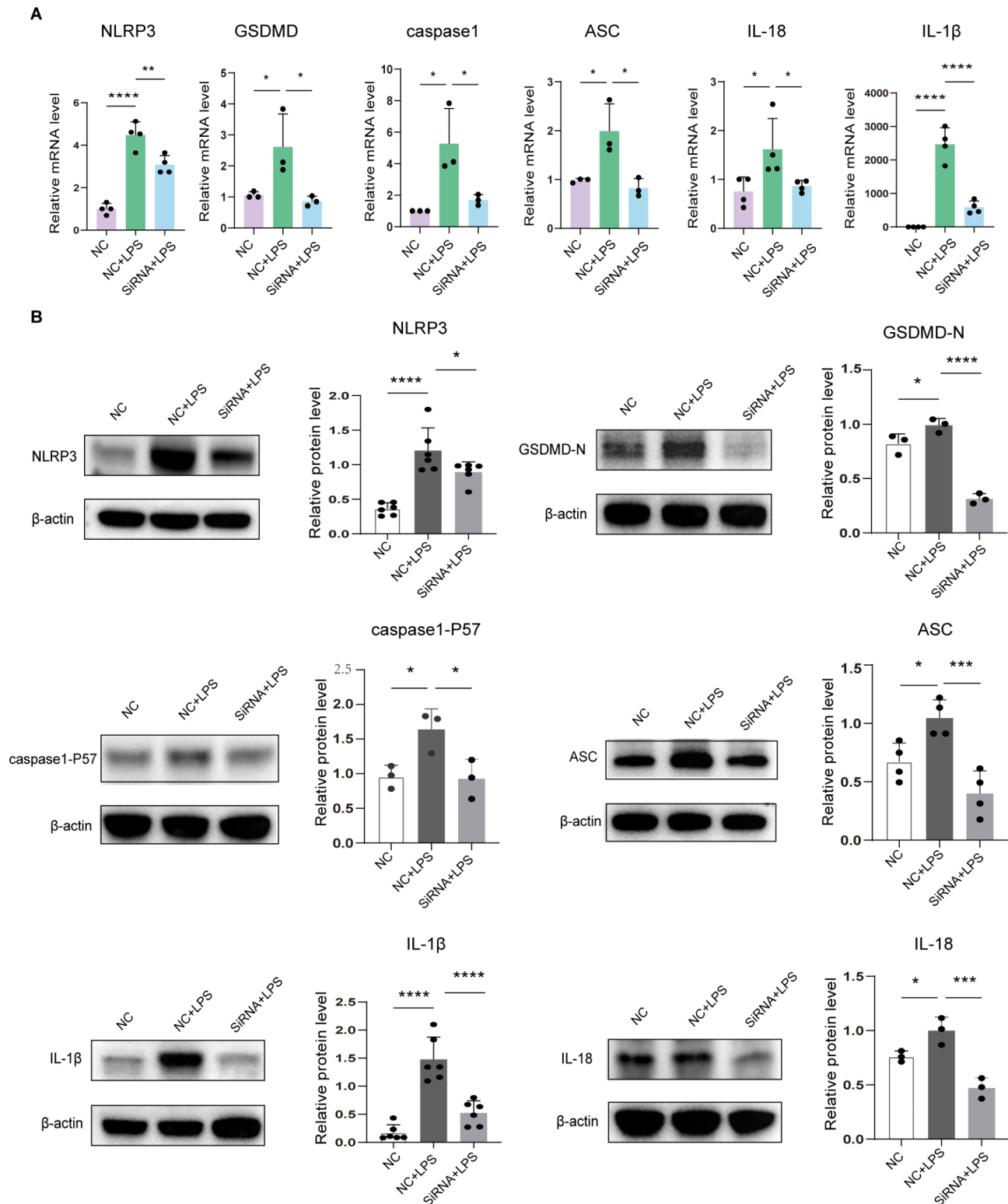


Fig. 7 OPN-siRNA inhibits pyroptosis in MH-s cells treated with LPS. **(A)** The mRNA expression levels of NLRP3, GSDMD, caspase1, ASC, IL-1 β and IL-18 in MH-s cells. **(B)** Western blotting analysis of the relative expression of the NLRP3, GSDMD, caspase1, ASC, IL-1 β and IL-18 in MH-s cells. The data are presented as the means \pm standard deviations (S.D.). *** indicates a difference between groups. * p < 0.05, ** p < 0.01, *** p < 0.001, **** p < 0.0001. Osteopontin, OPN; NOD-, LRR- and pyrin domain-containing 3, NLRP3; Gasdermin D, GSDMD; apoptosis-associated speck-like protein containing a CARD, ASC; interleukin, IL; tumour necrosis factor, TNF; negative control, NC; Small interfering RNA, siRNA; lipopolysaccharide, LPS; Mouse alveolar macrophage cells, MH-s; Quantitative Real-time reverse transcriptase-polymerase chain reaction, qPCR

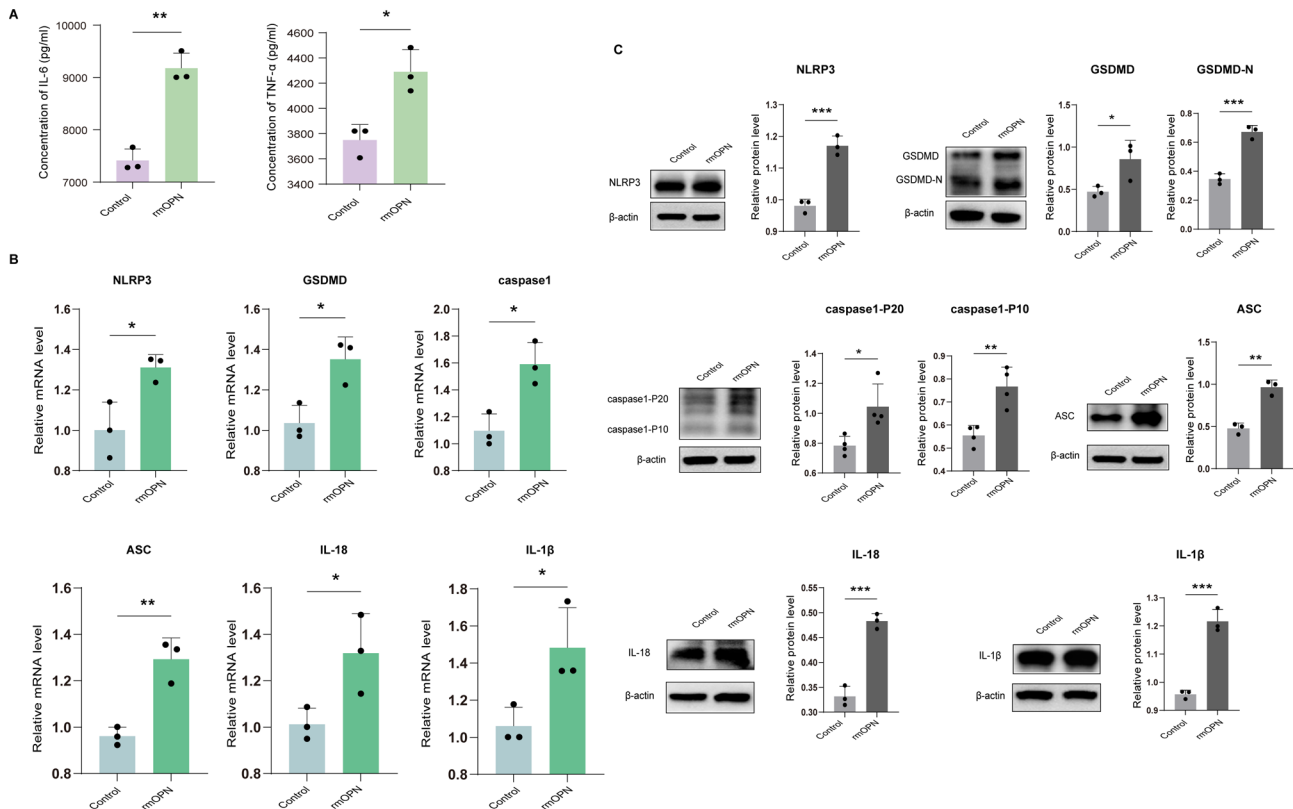


Fig. 8 rmOPN was supplemented after OPN silencing, and the protective effects in MH-s cells treated with LPS were reversed. **(A)** ELISAs were used to detect the concentration of IL-6 and TNF-α in cell supernatant of MH-s cells. **(B)** The mRNA expression levels of NLRP3, GSDMD, caspase1, ASC, IL-1β and IL-18 in MH-s cells. **(C)** Western blotting analysis of the relative expression of the NLRP3, GSDMD, caspase1, ASC, IL-1β and IL-18 in MH-s cells. The data are presented as the means ± standard deviations (S.D.). “***” indicates a difference between groups. * $p < 0.05$, ** $p < 0.01$, *** $p < 0.001$, **** $p < 0.0001$. Osteopontin, OPN; recombinant mouse OPN, rmOPN; interleukin, IL; tumour necrosis factor, TNF; NOD-, LRR- and pyrin domain-containing 3, NLRP3; Gasdermin D, GSDMD; apoptosis-associated speck-like protein containing a CARD, ASC; lipopolysaccharide, LPS; Mouse alveolar macrophage cells, MH-s; enzyme-linked immunosorbent assay, ELISA; Quantitative Real-time reverse transcriptase-polymerase chain reaction, qPCR

protein kinase (ERK) [18]. In previous research, OPN has been demonstrated to function as a proinflammatory cytokine and chemotactic agent, facilitating the migration of immune cells to areas of inflammation [7, 19–22]. Nonetheless, the majority of research have focused on the role of OPN on migration and activation [18, 23, 24], there is a lack of investigation into whether there is a correlation between OPN and the programmed cell death of macrophages. In our study, we found that macrophage infiltration and NLRP3 inflammasome expression in the lungs of septic mice were elevated compared to that in the sham group, and the use of OPN inhibitors could significantly ameliorate this situation. Correspondingly, previous studies have indicated that macrophage pyroptosis plays a crucial role in sepsis-induced lung injury by propagating the pulmonary inflammatory response, vascular leakage, and facilitating neutrophil migration to the lungs [25]. We have presented the initial evidence indicating a connection between pyroptosis in sepsis-related lung injury and OPN. In line with our results, OPN has been shown to be up-regulated in bleomycin-induced

pulmonary fibrosis and is associated with macrophage pyroptosis through elevated expression of multiple endocrine neoplasia type 1 (Men1) expression [26]. Likewise, when researchers employed calcium oxalate monohydrate (COM) to establish a nephrolithiasis cell model of macrophages, they observed that the expression trends of OPN and macrophage pyroptosis signaling pathways were notably consistent [27]. However, it remains ambiguous whether OPN is associated with macrophage pyroptosis, and the precise mechanism remains unclear. In our study, we observed that silencing OPN expression in MH-s cells can significantly reduce both the mRNA and protein levels of NLRP3, GSDMD, caspase-1, ASC, IL-1β and IL-18 in LPS-induced elevated pyroptosis pathway. Conversely, when rmOPN was administered following the silencing of OPN, the protective effects observed in MH-s cells treated with LPS were negated. Therefore, it can be concluded that preventing OPN-induced pyroptosis could potentially mitigate the inflammatory damage associated with sepsis. The present investigation has several limitations that deserve consideration. Firstly, it is a

single-center study with a relatively small sample size of sepsis patients. Furthermore, there is a lack of comparative analysis of OPN levels between survivors and non-survivors, as well as between sepsis patients and those with other organ dysfunctions in the PICU, highlighting the necessity for extensive clinical trials and additional research to elucidate the specific differential role of OPN in sepsis patients.

In summary, the findings of this study highlight the detrimental role of OPN in the context of sepsis. Moreover, the therapeutic administration of OPN inhibitors has been demonstrated to increase survival rates and attenuate lung injury in septic mice. Additionally, the protective mechanism of OPN inhibitors encompasses both anti-inflammatory effects and the suppression of pyroptosis. Consequently, OPN not only holds potential as a promising diagnostic marker for sepsis but also presents a novel therapeutic target for the development of sepsis treatment medications.

Abbreviations

OPN	Osteopontin
SPP1	Secreted phosphoprotein 1
CLP	Cecal ligation and puncture
LPS	Lipopolysaccharide
MH-S	Mouse Hemophagocytic Synuclein
PICU	Pediatric intensive care unit
WT	Wild-type
FBS	Fetal bovine serum
NC	Negative control
siRNA	Small interfering RNA
OI	OPN inhibitor
rmOPN	Recombinant mouse OPN
PBS	Phosphate buffered saline
ELISA	Enzyme-linked immunosorbent assay
TNF- α	Tumor necrosis factor-alpha
IL-6	Interleukin-6
IL-1 β	Interleukin-1 beta
LPS	Lipopolysaccharide
D/W	Dry-to-wet
PBST	Phosphate buffer saline with tween-20
DAPI	4',6-diamidino-2-phenylindole
H&E	Hematoxylin and eosin
qPCR	Real-time quantitative PCR
GAPDH	Glyceraldehyde-3-phosphate dehydrogenase
RIPA	Radioimmunoprecipitation assay
PMSF	Phenylmethanesulfonyl fluoride
SDS-PAGE	Sodium dodecyl sulfate-polyacrylamide
PVDF	Polyvinylidene fluoride
NLRP3	NOD-, LRR- and pyrin domain-containing 3
GSDMD	Gasdermin D
ASC	Apoptosis-related spot-like protein

Acknowledgements

Not applicable.

Author contributions

XF and LJ contributed to the conception and design. QW performed the experiments, analysed data, and wrote the manuscript. ZCY helped to revise the manuscript. ZXS, XL, ZL, and DDP helped in the acquisition of clinical data. All authors read and approved the final manuscript.

Funding

This research was supported by the Key Program of Chongqing Clinical Medical Research (Grant No. NCRCCHD-2021-KP-03) and the Program For

Youth Innovation in Future Medicine of Chongqing Medical University (W0124 to JL).

Data availability

No datasets were generated or analysed during the current study.

Declarations

Ethics approval and consent to participate

All procedures performed in studies involving human participants were approved by the Clinical Research Ethics Committee of Institutional Review Board of Children's Hospital of Chongqing Medical University (File No: (2021) Ethical Review Research No. 325-1). All animal experiments were conducted under the rules approved by the Ethics Committee of Chongqing Experimental Animal Center and the Animal Committee of Children's Hospital (CHCMU-IACUC20231208004).

Consent for publication

All listed authors consent to the submission, and all data are used with the consent of the person generating the data.

Competing interests

The authors declare no competing interests.

Author details

¹Department of Critical Care Medicine, Children's Hospital of Chongqing Medical University, Chongqing, China

²National Clinical Research Center for Child Health and Disorders, Chongqing, China

³Ministry of Education Key Laboratory of Child Development and Disorders, Chongqing, China

⁴Chongqing Key Laboratory of Pediatrics, Chongqing, China

⁵Department of Pediatric Intensive Care Unit, First Affiliated Hospital of Xixiang Medical University, Xixiang, China

⁶Department of Life Science Center, The First Affiliated Hospital of Xixiang Medical University, Xixiang, China

⁷Clinical Laboratory of Children's Hospital of Chongqing Medical University, Chongqing, China

⁸Department of Emergency, Children's Hospital of Chongqing Medical University, Chongqing, China

⁹Department of Pediatric Intensive Care Unit, Children's Hospital, Chongqing Medical University, Chongqing 400014, China

Received: 12 November 2024 / Accepted: 19 January 2025

Published online: 24 January 2025

References

1. Singer M, Deutschman CS, Seymour CW, Shankar-Hari M, Annane D, Bauer M, et al. The Third International Consensus definitions for Sepsis and septic shock (Sepsis-3). *JAMA*. 2016;315:801–10.
2. Liu R, Yu Z, Xiao C, Xu F, Xiao S, He J, et al. Epidemiology and clinical characteristics of pediatric sepsis in PICUs in Southwest China: a prospective multicenter study. *Pediatr Crit Care Med*. 2024;25:425–33.
3. Watson RS, Carrol ED, Carter MJ, Kissoon N, Ranjit S, Schlapbach LJ. The burden and contemporary epidemiology of sepsis in children. *Lancet Child Adolesc Health*. 2024;8:670–81.
4. International Consensus Criteria for Pediatric Sepsis and Septic Shock. - PMC [Internet]. [cited 2024 Aug 11]. Available from: <https://www.ncbi.nlm.nih.gov/pmc/articles/PMC10900966/>
5. Global regional, and national sepsis incidence and mortality, 1990–2017: analysis for the Global Burden of Disease Study - PMC [Internet]. [cited 2024 Sep 10]. Available from: <https://www.ncbi.nlm.nih.gov/pmc/articles/PMC6970225/>
6. Icer MA, Gezmen-Karadag M. The multiple functions and mechanisms of osteopontin. *Clin Biochem*. 2018;59:17–24.
7. Bastos ACSda, Gomes F, Silva AVP, Emerenciano GR, Ferreira M, Gimba LB. ERP: The intracellular and secreted sides of Osteopontin and their putative physiopathological roles. *Int J Mol Sci*. 2023;24.

8. Lund SA, Wilson CL, Raines EW, Tang J, Giachelli CM, Scatena M. Osteopontin mediates macrophage chemotaxis via α_4 and α_9 integrins and survival via the α_4 integrin. *J Cell Biochem*. 2013;114:1194–202.
9. Zou C, Luo Q, Qin J, Shi Y, Yang L, Ju B, et al. Osteopontin promotes mesenchymal stem cell migration and lessens cell stiffness via integrin $\beta 1$, FAK, and ERK pathways. *Cell Biochem Biophys*. 2013;65:455–62.
10. Miyazaki T, Ono M, Qu W-M, Zhang M-C, Mori S, Nakatsuru S, et al. Implication of allelic polymorphism of osteopontin in the development of lupus nephritis in MRL/lpr mice. *Eur J Immunol*. 2005;35:1510–20.
11. Kawamura K, Iyonaga K, Ichiyasu H, Nagano J, Suga M, Sasaki Y. Differentiation, maturation, and survival of dendritic cells by osteopontin regulation. *Clin Diagn Lab Immunol*. 2005;12:206–12.
12. Vaschetto R, Nicola S, Olivieri C, Boggio E, Piccolella F, Mesturini R, et al. Serum levels of osteopontin are increased in SIRS and sepsis. *Intensive Care Med*. 2008;34:2176–84.
13. DeJager L, Pinheiro I, Dejonckheere E, Libert C. Cecal ligation and puncture: the gold standard model for polymicrobial sepsis? *Trends Microbiol*. 2011;19:198–208.
14. Linkermann A, Stockwell BR, Krautwald S, Anders H-J. Regulated cell death and inflammation: an auto-amplification loop causes organ failure. *Nat Rev Immunol*. 2014;14:759–67.
15. Carbone F, Bonaventura A, Vecchiè A, Meessen J, Minetti S, Elia E, et al. Early osteopontin levels predict mortality in patients with septic shock. *Eur J Intern Med*. 2020;78:113–20.
16. Castello LM, Baldrighi M, Molinari L, Salmi L, Cantaluppi V, Vaschetto R et al. The role of Osteopontin as a Diagnostic and Prognostic Biomarker in Sepsis and Septic Shock. *Cells*. 2019;8.
17. Zhong J, Eckhardt ERM, Oz HS, Bruemmer D, de Villiers WJS. Osteopontin deficiency protects mice from dextran sodium sulfate-induced colitis. *Inflamm Bowel Dis*. 2006;12:790–6.
18. Hirano Y, Aziz M, Yang W-L, Wang Z, Zhou M, Ochani M, et al. Neutralization of osteopontin attenuates neutrophil migration in sepsis-induced acute lung injury. *Crit Care*. 2015;19:53.
19. Clemente N, Raineri D, Cappellano G, Boggio E, Favero F, Soluri MF, et al. Osteopontin bridging Innate and Adaptive Immunity in Autoimmune diseases. *J Immunol Res*. 2016;2016:7675437.
20. Lamort A-S, Giopanou I, Psallidas I, Stathopoulos GT. Osteopontin as a link between inflammation and Cancer: the Thorax in the spotlight. *Cells*. 2019;8.
21. Intracellular osteopontin regulates homeostasis and function of natural killer cells - PubMed [Internet]. [cited 2023 Jun 17]. Available from: <https://pubmed.ncbi.nlm.nih.gov/25550515/>
22. Tan Y, Zhao L, Yang Y-G, Liu W. The role of Osteopontin in Tumor Progression through Tumor-Associated macrophages. *Front Oncol*. 2022;12:953283.
23. Weber GF, Zawaideh S, Hikita S, Kumar VA, Cantor H, Ashkar S. Phosphorylation-dependent interaction of osteopontin with its receptors regulates macrophage migration and activation. *J Leukoc Biol*. 2002;72:752–61.
24. Kim D, Haynes CL. The role of p38 MAPK in neutrophil functions: single cell chemotaxis and surface marker expression. *Analyst*. 2013;138:6826.
25. Qin X, Zhou Y, Jia C, Chao Z, Qin H, Liang J, et al. Caspase-1-mediated extracellular vesicles derived from pyroptotic alveolar macrophages promote inflammation in acute lung injury. *Int J Biol Sci*. 2022;18:1521–38.
26. Lu Y, Zhao J, Tian Y, Shao D, Zhang Z, Li S, et al. Dichotomous roles of Men1 in macrophages and fibroblasts in Bleomycin—Induced Pulmonary Fibrosis. *Int J Mol Sci*. 2022;23:5385.
27. Ding T, Zhao T, Li Y, Liu Z, Ding J, Ji B, et al. Vitexin exerts protective effects against calcium oxalate crystal-induced kidney pyroptosis in vivo and in vitro. *Phytomedicine*. 2021;86:153562.

Publisher's note

Springer Nature remains neutral with regard to jurisdictional claims in published maps and institutional affiliations.